

MINIMUM VARIANCE ADAPTIVE BEAMFORMING IN ACTIVE SONAR IMAGING

Safiye Dursun^a, Andreas Austeng^a, Roy E Hansen^{a,b}, Sverre Holm^a

^aDepartment of Informatics, University of Oslo, Norway.

^bNorwegian Defence Research Establishment, P O Box 25, NO-2027 Kjeller, Norway

Contact author: A. Austeng, Dept. of Informatics, Univ. of Oslo, P.O.Box 1080, Blindern, NO-0136 Oslo, Norway. Fax: +47 22 85 24 01. Email:

Andreas.Austeng@ifi.uio.no.

Abstract: *The delay-and-sum (DAS) beamformer is commonly used in active sonar imaging. The large sidelobes of the DAS beamformer can be suppressed using aperture shading. This gives lower sidelobe levels at the cost of a wider mainlobe. The minimum variance (MV) beamformer uses the received data to adjust the weights of each receiving element to produce the least total output power while maintaining unit gain in the view direction. This suppresses signals from off-axis directions and allows large sidelobes in directions with no signal. We have developed and applied a robust MV beamformer to the Kongsberg Maritime HISAS 1030 sonar, which is an active sonar system. The transmitted signal was a 30 kHz band centered at 100 kHz and we used one 32 element receiving array. We first applied the MV and DAS beamformers to a simulated dataset. MV beamforming of two closely spaced reflectors showed better resolution and suppression of sidelobe levels compared to DAS. On a simulated scene with speckle, highlight and shadow the MV beamformer showed better lateral edge definition at the cost of slightly lower contrast. We also demonstrate these effects of the MV adaptive beamformer on real data collected by the HUGIN autonomous underwater vehicle carrying a HISAS 1030 sonar.*

Keywords: *Beamforming, Adaptive beamforming, Capon, Minimum variance, MVDR, High resolution imaging, Sonar.*

1. INTRODUCTION

To focus an array of sensors towards a specific direction or point in space is known as beamforming. The standard beamforming method used in sonar imaging is delay-and-sum (DAS). Control of the sidelobe level of the DAS beamformer can be achieved by using aperture shading. This results in increased contrast at the expense of resolution. An adaptive beamformer uses the recorded wavefield to compute the aperture shading. Increased resolution can be achieved since an adaptive beamformer can suppress interfering signals from off-axis directions and allow larger sidelobes in directions in which there is no received energy. Adaptive beamforming methods such as the minimum variance (MV) beamformer [2], also known as Capon or Minimum Variance Distortionless Response (MVDR) beamformer, have successfully been used in passive wideband sonar imaging [1], and more recently been adopted to active wideband sonar imaging [3,4].

Systems with active transmission cause coherent received echoes. The standard MV beamformer assumes incoherent echoes. For simple scenarios like single point targets, the echoes will be incoherent. For more complex scenarios, the returning echoes are coherent and several measures need to be taken in order to handle this. These measures are various forms of averaging and smoothing of the estimates.

In this work we have applied the MV beamformer to simulated and real data. We have shown that by addressing the problems of coherence, the performance of the MV beamformer in an active imaging system is better or comparable with that of the DAS beamformer.

In the following section, a brief introduction to the MV beamformer is given. In Section 3, the simulation and experimental results are presented and discussed. A conclusion is drawn in Section 4.

2. METHODS

For both the DAS and MV beamformers we assume an array of M elements, each recording signal $x_m[n]$. The output of the beamformer, $z[n]$, is a weighed sum of the time-delayed M measurements

$$z[n] = \sum_{m=0}^{M-1} w_m[n] x[n - \Delta_m] = \mathbf{w}^H[n] \mathbf{X}[n], \quad (1)$$

where Δ_m is the time delay applied to signal m , $w_m[n]$ is the weight applied to sensor m at time n , $\mathbf{w}^H[n] = [w_0[n] \cdots w_{M-1}[n]]$ and $\mathbf{X}[n] = [x_0[n - \Delta_0] \cdots x_{M-1}[n - \Delta_{M-1}]]^T$.

In the DAS beamformer the weights are independent of the received signal. We have used either a uniform or a smooth window with tapered edges. A smoothed window gives a lower sidelobe-level and a wider main lobe compared to a uniform window.

In the Capon beamformer the weights are calculated from the recorded signal by minimizing the variance (power) of $z[n]$ while maintaining unit gain at the focal point. This gives unique weights for all depths and viewing angles. The analytical solution of to the problem is given by [2]:

$$\mathbf{w}[n] = \frac{\mathbf{R}^{-1}[n] \mathbf{a}}{\mathbf{a}^H \mathbf{R}^{-1} \mathbf{a}}, \quad (2)$$

where $\mathbf{R}[n]$ is the spatial covariance matrix and \mathbf{a} is the steering vector.

In order to calculate these weights, the spatial covariance matrix has to be estimated. To estimate an invertible spatial covariance matrix from realistic signals, $\mathbf{R}[n]$ in (2),

both averaging of the observed signals in temporal and spatial domains as well as regularization is required. In the spatial domain, averaging is performed by dividing the aperture into (overlapping) subarrays and averaging the spatial covariance matrices of each subarray. The general covariance matrix estimate averaged over $2K+1$ temporal samples and $M-L+1$ subarrays of length L is given by:

$$\hat{\mathbf{R}}[n] = \varepsilon \mathbf{I} + \tilde{\mathbf{R}}[n] \text{ where } \tilde{\mathbf{R}}[n] = \frac{1}{(2K+1)(M-L+1)} \sum_{k=-K}^K \sum_{l=0}^{M-L} \mathbf{X}_l[n-k] \mathbf{X}_l^H[n-k], \quad (3)$$

$\mathbf{X}_l[n] = [x_l[n-\Delta_l] \cdots x_{l+L-1}[n-\Delta_{l+L-1}]]^T$, \mathbf{I} is the identity matrix and ε is a constant. We have chosen this constant to be proportional to the power of the received data, i.e. $\varepsilon = \text{tr}[\tilde{\mathbf{R}}[n]] \cdot \delta / L$, where $\text{tr}\{\cdot\}$ is the trace operator and δ is typically less than 1. A more thorough description of the algorithm, the estimation of the covariance matrix and the choice of parameters can be found in [5,6].

3. RESULTS AND DISCUSSION

We have simulated the Kongsberg Maritime HISAS 1030 sonar [7] with one transmitter and a 32 element linear receive array operating at 100 kHz. First we simulated a number of pairwise reflectors located at 50 and 70 meters range. The reflectors were separated by one meter. Fig. 1 shows the fields obtained using the DAS beamformer with rectangular and Kaiser 3.5 window shading, and the MV beamformer using a subarray length of 12 and diagonal loading with $\delta=0.2$. The covariance matrix has been averaged over one wavelength in time. These parameters have been used for all MV images.

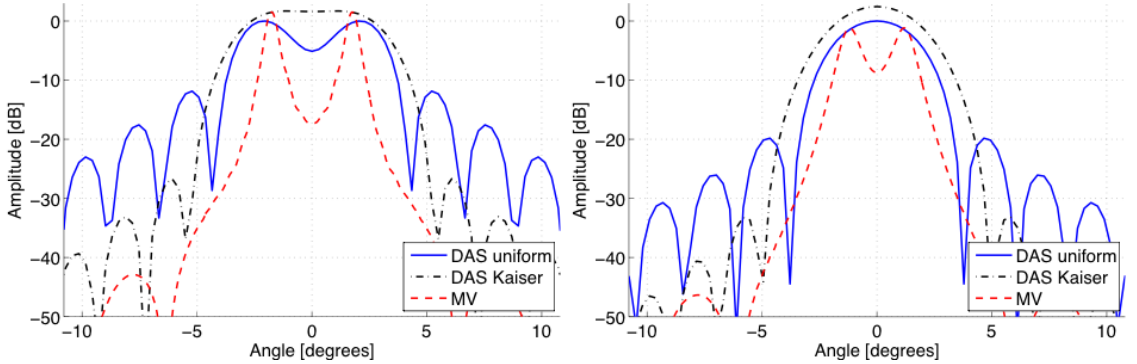


Fig. 1: Cut trough focus at 50 meters (to the left) and at 70 meter (to the right) of two point reflectors separated by one meter.

At 50 meters range, we see that the DAS beamformer with a rectangular window and the MV beamformer are able to resolve the two reflectors, while DAS shaded with a Kaiser window cannot resolve them. At 70 meters range, only the Capon method can resolve the reflectors. The sidelobe level of the MV beamformer are seen to be much lower than both the DAS beamformer with and without shading, and the width of the point response for the MV beamformer is much narrower than for the two others.

We have further simulated a scene with speckle, highlight and shadow. Simulated images from the same choice of beamformers are shown in Fig. 2. The images are normalized such that the mean intensity level is the same in the speckle region. The highlight region is in these images indicated with a white ring. Fig. 3 shows averaged

cuts through the highlight and shadow regions. In the highlight, the response is averaged over a 0.6 meter wide band while in the shadow region the response from 43.5 to 45.5 meter is averaged. Fig. 4 shows averaged axial cuts through the centre of both the speckle, highlight and shadow regions. The response is averaged over a 0.6 meter wide band.

Fig. 2 shows that compared to the DAS beamformer, the MV beamformer produces images with better definition of both the highlight and the shadow region at a possible cost of a slightly lower contrast. Studying the details of these images as given in Fig. 3, the response for the MV beamformer in the highlight region has approximately 1-2 dB lower amplitude than the DAS beamformers. The true value of the highlight region should have been constant and at 15.6 dB. All the beamformers show a large variation in the amplitude response. The DAS beamformers seem to overestimate while the MV beamformer seems to underestimate the response. The width of the highlight region is overestimated for the DAS beamformers compared to the MV beamformer, the Kaiser shaded DAS beamformer producing the widest response. This result is in agreement with the simulated point reflector results given above. In the shadow region, the edges are best preserved by the MV beamformer. The filling of the shadow region is more severe for the DAS beamformer with rectangular shading compared to the two other. The axial cut given in

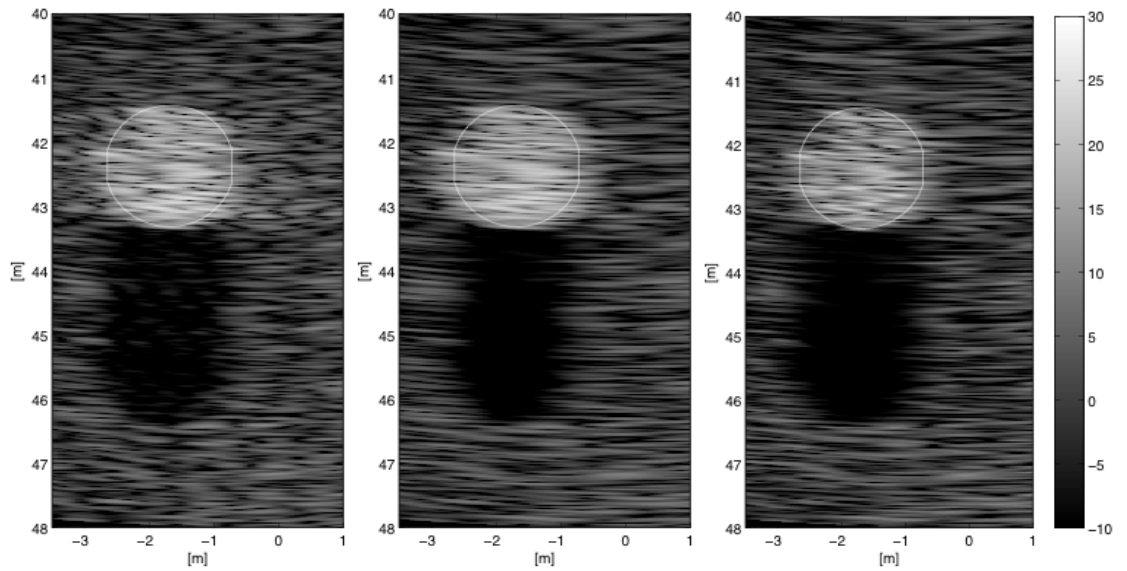


Fig. 2: Simulated images of speckle, highlight and shadow. DAS with rectangular shading (left), DAS with Kaiser shading (middle) and MV (right).

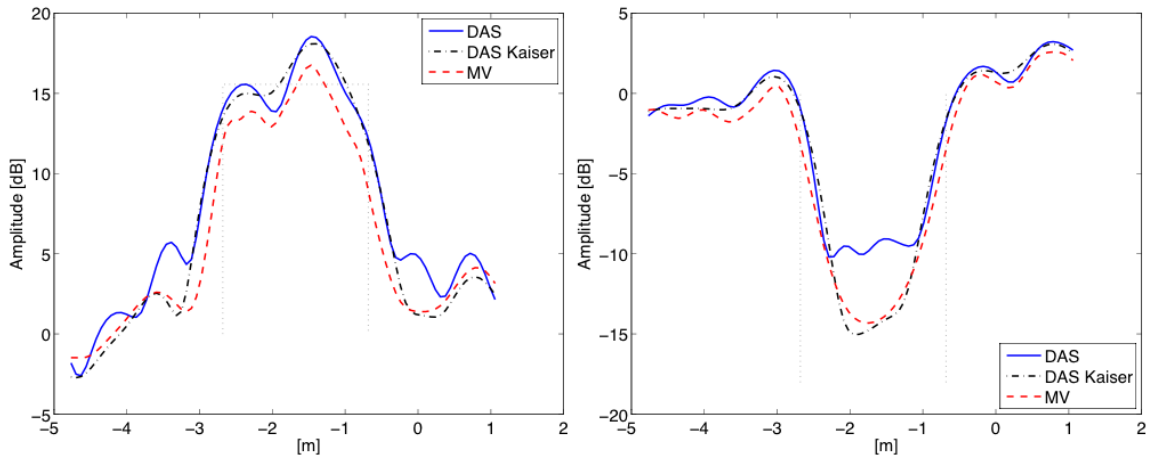


Fig. 3: Lateral cut through highlight (to the left) and shadow (to the right) for different choices of beamformer; DAS with rectangular shading, DAS with Kaiser shading and MV.

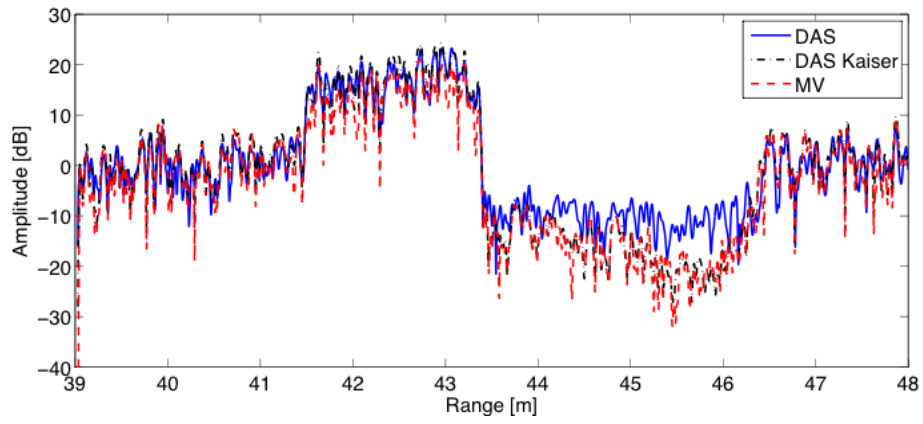


Fig. 4: Axial cut through speckle, highlight and shadow for different choices of beamformer; DAS with rectangular shading, DAS with Kaiser shading and MV.

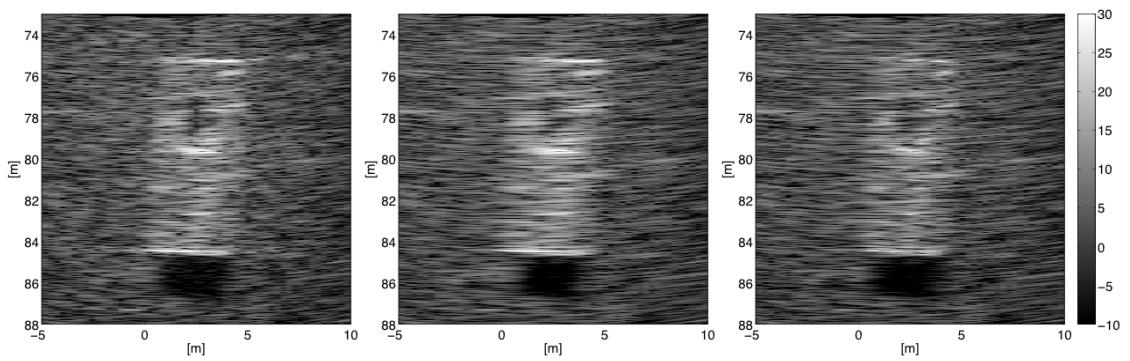


Fig. 5: Images of a barge from the HISAS 1030 sonar for different choices of beamformer; DAS with rectangular shading (left), DAS with Kaiser shading (middle) and MV (right).

Fig. 4 shows that the response for the MV beamformer are close to the response of the Kaiser shaded DAS beamformer, and for most depths lower than the response for the rectangular shaded DAS beamformer.

Fig. 5 shows images from real data from HISAS 1030 [7], processed using the three different beamformers. Note that this is a sectorscan image, i.e. an image from a single ping. This is not to be confused with sidescan sonar images or synthetic aperture sonar images that are based on multiple pings. The images show a barge throwing a short shadow. As for the simulated images, the MV beamformer produces the image with the narrowest highlight region. The width of the shadow region is as wide as for the DAS beamformer with rectangular shading, but the filling of the shadow is not as severe and comparable with the DAS beamformer with Kaiser shading.

4. CONCLUSION

We have presented sonar images from simulated and real data. The images have been produced using three different choices of beamformers, DAS with rectangular shading, DAS with Kaiser shading and MV. We have shown that the MV beamformer produces edge responses that are better or comparable with a DAS beamformer without shading and a sidelobe level or filling of shadow region which is comparable to a Kaiser weighted DAS beamformer.

ACKNOWLEDGEMENTS

We kindly thank Kongsberg Maritime for providing experimental data from the HISAS 1030 sonar.

BIBLIOGRAPHY

- [1] **Vaccaro, R.J.**, "The past, present, and the future of underwater acoustic signal processing," *Signal Processing Magazine, IEEE* , vol.15, no.4, pp.21-51, July 1998.
- [2] **Capon, J.**, "High-resolution frequency-wavenumber spectrum analysis," *Proc. IEEE*, vol. 57, pp. 1408-1418, August 1969.
- [3] **Lo, K.W.**, "Adaptive array processing for wide-band active sonars," *Oceanic Engineering, IEEE Journal of* , vol.29, no.3, pp. 837-846, July 2004.
- [4] **Ferguson, B.G., Lo, K.W., and Wyber, R.J.**, "Advances in High-Frequency Active Sonars for Countering Asymmetric Threats in Littoral Waters," *OCEANS 2006* , vol., no., pp.1-6, 18-21 Sept. 2006.
- [5] **Synnevag, J.-F., Austeng, A., and Holm, S.**, "Adaptive Beamforming Applied to Medical Ultrasound Imaging," *Ultrasonics, Ferroelectrics and Frequency Control, IEEE Transactions on* , vol.54, no.8, pp.1606-1613, August 2007.
- [6] **Holm, S., Synnevag, J.-F., and Austeng, A.**, "Capon Beamforming for Active Ultrasound Imaging Systems," *Digital Signal Processing Workshop and 5th IEEE Signal Processing Education Workshop, 2009. DSP/SPE 2009. IEEE 13th* , pp.60-65, 4-7 Jan. 2009.
- [7] **Hansen, R.E., Callow, H.J., Sæbø, T.O., Synnes, S.A., Hagen, P.E., Fossum, T.G., and Langli, B.**, "Synthetic aperture sonar in challenging environments: Results from HISAS 1030", In *Proceedings of Underwater Acoustic Measurements 2009*, Nafplion, Greece, June 2009